



Published in final edited form as:

Osteoarthritis Cartilage. 2023 July ; 31(7): 908–918. doi:10.1016/j.joca.2023.02.072.

CAMKK2 is Upregulated in Primary Human Osteoarthritis and its Inhibition Protects Against Chondrocyte Apoptosis

Julian E. Dilley, MD^{1,2,3,@}, Abhijit Seetharam, MD^{1,2,3,@}, Xinchun Ding, PhD^{1,3}, Margaret A. Bello, BS^{1,3}, Jennifer Shutter, MS^{1,3}, David B. Burr, PhD^{1,3}, Roman M. Natoli, MD, PhD^{2,3}, Todd O. McKinley, MD^{1,2,3}, Uma Sankar, PhD^{1,3,*}

¹Department of Anatomy, Cell Biology and Physiology, Indiana University School of Medicine, Indianapolis, IN, 46202, USA

²Department of Orthopaedic Surgery, Indiana University School of Medicine, Indianapolis, IN, 46202, USA

³Indiana Center for Musculoskeletal Health, Indiana University School of Medicine, Indianapolis, IN 46202, USA.

Abstract

Objective: To investigate the role of calcium/calmodulin-dependent protein kinase kinase 2 (CAMKK2) in human osteoarthritis.

Materials and Methods: Paired osteochondral plugs and articular chondrocytes were isolated from the relatively healthier (intact) and damaged portions of human femoral heads collected from patients undergoing total hip arthroplasty for primary osteoarthritis (OA). Cartilage from femoral plugs were either flash frozen for gene expression analysis or histology and immunohistochemistry. Chondrocyte apoptosis in the presence or absence of CAMKK2 inhibition was measured using flow cytometry. CAMKK2 overexpression and knockdown in articular chondrocytes were achieved via Lentivirus- and siRNA-mediated approaches respectively, and their effect on pro-apoptotic and cartilage catabolic mechanisms was assessed by immunoblotting.

Results: CAMKK2 mRNA and protein levels were elevated in articular chondrocytes from human OA cartilage compared to paired healthier intact samples. This increase was associated with elevated catabolic marker matrix metalloproteinase 13 (MMP-13), and diminished anabolic markers aggrecan (ACAN) and type II collagen (COL2A1) levels. OA chondrocytes displayed

*Address correspondences to: Uma Sankar, Ph.D., 635 Barnhill Drive, MS-5055, Indianapolis, IN 46202 USA. Tel: (317) 274-7870, Fax: (317) 856-5710; usankar@iu.edu.

@JD and AS contributed equally to this study.

Author contributions

AS, JED, XD, JAS and MB designed and performed experiments and analyzed data; JED and AS prepared figures; JED wrote the manuscript; US; XD and JED drafted the manuscript; US conceived and supervised the study, analyzed data and drafted the manuscript; RN, TM and DBB provided critical input on data interpretation and edited the manuscript.

Conflict of interest

All authors of this manuscript state that they have no conflict of interest. The authors further state that there are no restrictions on full access for all authors to all raw data, statistical analyses and material used in the study reported in this manuscript.

Publisher's Disclaimer: This is a PDF file of an unedited manuscript that has been accepted for publication. As a service to our customers we are providing this early version of the manuscript. The manuscript will undergo copyediting, typesetting, and review of the resulting proof before it is published in its final form. Please note that during the production process errors may be discovered which could affect the content, and all legal disclaimers that apply to the journal pertain.

enhanced apoptosis, which was suppressed following pharmacological inhibition of CAMKK2. Levels of MMP13, pSTAT3, and the pro-apoptotic marker BAX became elevated when CAMKK2, but not its kinase-defective mutant was overexpressed, whereas knockdown of the kinase decreased the levels of these proteins.

Conclusions: CAMKK2 is upregulated in human OA cartilage and is associated with elevated levels of pro-apoptotic and catabolic proteins. Inhibition or knockdown of CAMKK2 led to decreased chondrocyte apoptosis and catabolic protein levels, whereas its overexpression elevated them. CAMKK2 may be a therapeutic target to prevent or mitigate human OA.

Keywords

Osteoarthritis; CAMKK2; chondrocyte; apoptosis; catabolism

Introduction:

Osteoarthritis (OA) of the knee and hip is a leading cause of disability worldwide with a symptomatic prevalence of 12-16% and 6-17% respectively, worldwide¹. To date, there are no effective treatments to prevent or mitigate the progression of OA. The current gold standard for end stage OA management is total knee and hip arthroplasty. Treatment of hip and knee OA with arthroplasty costs \$12,381-\$13,771 per affected Medicare beneficiary², and although mostly successful, arthroplasty can have costly and morbid complications³. OA affects the whole joint compartment including the synovium, subchondral bone, and articular cartilage. It is characterized by synovial inflammation, meniscal and ligamentous degeneration, osteophyte formation, subchondral bone remodeling, and articular cartilage degradation^{4,5}.

Joint instability leads to upregulation of inflammatory cytokines IL-1 β and IL-6 from chondrocytes and synovial macrophages. These inflammatory cytokines induce chondrocytes to upregulate the synthesis of metalloproteinases (MMPs), such as MMP-13, which degrade articular cartilage, resulting in an overall catabolic environment of articular cartilage⁶. Thus, in primary OA, subtle structural abnormalities causing minor stress aberrations within the joint accumulate over time. Collectively, these seemingly different inciting events funnel into several common pathologic pathways that include apoptosis⁷⁻⁹. Chondrocyte apoptosis has been shown to be mediated by BAX, a proapoptotic protein of the BCL-2 family^{10,11}. Under normal conditions, BCL-2 maintains BAX in the cytosol, and the oligomerization of BAX proteins in the mitochondrial outer membrane is prevented. During times of cellular stress or activation of intrinsic apoptotic pathways, BAX oligomerizes at the mitochondrial outer membrane, increasing mitochondrial outer membrane permeability, which allows the release of cytochrome c and activation of downstream caspases, resulting in apoptosis¹⁰. Chondrocyte apoptosis progresses more rapidly in early OA than at later stages of the disease⁹. As the disease progresses, chondrocytes become increasingly sensitive to inflammation-mediated apoptosis¹². Increased chondrocyte apoptosis is associated with proteoglycan depletion and cartilage catabolism⁷ and has been shown to precede changes in subchondral bone remodeling¹³.

CAMKK2 is a serine/threonine protein kinase activated by Ca²⁺-bound calmodulin that phosphorylates downstream substrates such as CAMKIV and adenosine monophosphate-dependent protein kinase (AMPK)¹⁴. The CaMKK2/AMPK pathway is involved in metabolic responses and energy homeostasis in various cell types¹⁵. CAMKK2 is integral to macrophage synthesis of inflammatory cytokines in response to activation of toll like receptor 4 (TLR4)¹⁶. Recently, we reported a role for the kinase in a murine model of PTOA. Inhibition or deletion of murine CAMKK2 protected against synovial inflammation, subchondral bone remodeling, and cartilage catabolism¹⁷, all hallmarks of PTOA. However, whether CAMKK2 plays a role in human OA is hitherto unknown.

The aim of the current study is to determine if CAMKK2 is differentially expressed in human OA cartilage and evaluate the effect of its inhibition on chondrocyte viability and catabolism. We hypothesized that CAMKK2 is upregulated in OA cartilage tissue, correlating with elevated levels of chondrocyte catabolism, apoptosis, and decreased levels of anabolism, such that its inhibition will mitigate these OA-associated effects on chondrocytes.

Methods:

Human sample procurement and preparation:

All studies involving human osteochondral tissue and articular cartilage were approved by Indiana University Institutional Review Board (IRB ID 2003626223) and the DoD Human Research Protection Office (HRPO Log Number E01450.1a).

De-identified human femoral heads were collected from patients undergoing total hip arthroplasty (THA) for primary OA (Table 1). Radiography-based Kellgren-Lawrence grade 3 or lower OA severity was used as a cut off for femoral head collection, as those at stage 4 had a consistent lack of cartilage tissue¹⁸. We collected N=12 THA samples, 7 female and 5 male with age range of 44-76 (Table 1). With N=12 per group, at type I error level 0.05, we expected to have an 80% power to detect a mean difference as 0.9 times the SD for OARSI scoring. Femoral heads were immediately placed in sterile saline prior to processing. Paired osteochondral plugs were extracted from damaged (more loaded medial side) and relatively healthier (less loaded lateral posterior side) portions of each femoral head using a bone graft harvester instrument (AR-1981-10H, Arthrex Inc., Naples, FL). Two plugs were extracted from each location (Fig. 1). One set of plugs was immediately flash frozen for RNA isolation and quantitative reverse transcriptase polymerase chain reaction (qRT-PCR) analysis. The second set was fixed in neutral-buffered formalin, decalcified, embedded in paraffin, and sectioned (5 µm thickness) for histology and immunohistochemistry (IHC) (Fig. 1).

Histology and immunohistochemistry (IHC) of osteochondral specimens

Formalin-fixed femoral head plugs were decalcified in 14% EDTA (pH 7.4) and dehydrated before paraffin embedding. Five µm thick serial sections were stained with safranin O fast green (SO) and hematoxylin-eosin (H&E). OA severity was assessed using the Osteoarthritis Research Society International (OARSI) scoring system in a blinded manner

on SO-stained serial sections on a scale ranging from 0 to 6 for parameters such as chondrocyte death, hypertrophy, chondrocyte cloning, loss of SO staining, surface fibrillation and bone alterations¹⁹⁻²².

Terminal deoxynucleotidyl transferase dUTP nick end labeling (TUNEL) assay was performed on serial sections using the TUNEL Chromogenic Apoptosis Detection Kit (ABP Bioscience, Rockville, MD), per manufacture's protocol, and counterstained with Gill No. 1 Hematoxylin (Millipore Sigma, Burlington, MA). Other IHC assays were performed per previous protocol²³ with primary antibodies indicated in Supplementary Table 1, and counterstained with hematoxylin. Images were captured using a Leica DMi8 microscope, processed with Leica LAS-X software (Leica CM1950, Wetzlar, Germany), and quantified by counting immunopositive and total cells within articular cartilage from 14 regions of interest (7 superficial and 7 deep regions) per sample using ImageJ (NIH, USA). Superficial regions were inclusive of the tangential and transitional layers of cartilage, and the deep regions were inclusive of the radial layer to the tide mark.

Quantitative reverse transcription polymerase chain reaction (qRT-PCR)

Flash frozen femoral head plugs from "healthier" intact and osteoarthritic areas of the femoral head were manually ground with mortar and pestle in the presence of liquid nitrogen and RNA was isolated utilizing Trizol and RNAqueous 4-PCR kit (both Invitrogen, Thermo Fisher) per the manufacturer's protocol. cDNA was generated using High-Capacity cDNA Reverse Transcription Kit (Invitrogen, Thermo Fisher). QRT-PCR was performed using iTaq™ Universal SYBR® Green Supermix on the CFX Connect™ Real-Time system (Bio-Rad Laboratories®, Hercules, CA, USA). PCR primers (Supplementary Table 2) were synthesized by Integrated DNA technologies (Coralville, IA, USA). Levels of mRNA were normalized to GAPDH and quantified using the Livak method²⁴.

Human articular chondrocyte isolation and culture

After plugs were extracted, cartilage tissue was harvested from the osteoarthritic and healthier portions of the same femoral head. Briefly, cartilage was shaved from the femoral head with a razor blade and then cut into 1x1x0.5 mm sections. Isolated cartilage was then digested with 2.5 mg/ml of Collagenase P and 2.5 mg/ml of Pronase (both Millipore Sigma, Burlington, MA) for 15 h at 37°C with shaking, in culture media (CM) containing DMEM:F12 supplemented with 2% penicillin/streptomycin (Thermo Fisher, Waltham, MA) and 10% fetal bovine serum (FBS). Cells were then seeded on a 6-well plate at a density of 0.8-1 million cells per well for expansion, and CM was changed every 48 hours. P0 chondrocytes were used in all experiments. To assess whether CaMKK2 levels are altered by inflammatory cytokines, P0 chondrocytes were serum starved for 12 h for synchronization, and then released into full media containing 10% FBS before treating with 10 ng/ml human recombinant IL-1β (Millipore Sigma) for 24 h.

Chondrocyte apoptosis assay:

P0 primary chondrocytes, isolated as above and seeded for 3 days, underwent treatment with or without 2 μM STO-609, a selective pharmacological inhibitor of CAMKK2, for 24 hours. STO-609 (TOCRIS Bioscience Ellisville, MO, USA), was prepared in 1X phosphate

buffered saline (PBS) as reported¹⁷. Where applicable, 1X PBS was used as control. Cells were then treated with Accutase (Innovative Cell Technologies, Inc., San Diego, CA) and washed twice with 1X PBS. The cells were then resuspended in cold PBS and labeled with Annexin V-PE (to identify apoptotic cells) and the fluorescent DNA marker 7-Aminoactinomycin D (7-ADD) (BD Pharmingen, PE Annexin V Apoptosis Detection Kit) per manufacturer instructions. After labeling, cells were analyzed using a BD LSR II Flow Cytometer (BD Biosciences).

Explant culture:

Osteochondral cores (2 cores each from 5 individual patients) were isolated from the OA part of THA samples with a KL grade of mostly 2 – four samples scored 2 and one scored 3 (Table 2). The cores/explants were then placed in culture media for 24 h. The OA explants taken from the same individual patient sample were “paired” such that one was treated with 1X PBS (Control) whereas the other one was treated with 8 μ M STO-609 for 24 or 48 h. Samples were then fixed in 4% paraformaldehyde (PFA) for 48 h, following by 70% ethanol, and then embedded in paraffin and cut into 5 μ m thick sections. STO-609-mediated inhibition of CaMKK2 enzyme function was evaluated by IHC of the explant sections using phospho (p) and total CAMKIV, a canonical substrate of CAMKK2. Apoptotic cells were evaluated by TUNEL assay as mentioned above. The average number of TUNEL-positive cells, calculated as a percentage of the total nuclei population were counted from 3 randomly selected fields of each sample under a Leica DMi8 fluorescent microscope (Leica CM1950, Wetzlar, Germany).

Lentiviral vector production and determination of virus titer

FLAG- rat (r) CaMKK2 (wild type, WT), or FLAG-rCaMKK2 D311A (mutant)^{25, 26} was cloned into the dual-promoter Lentivirus vector pCDH-MSCV-MCS-EF1-copGFP (System Biosciences (SBI), Mountain View, CA). Lentivirus particles were generated in 293T cells²⁷ by co-transfecting 18.75 μ g of pCDH Lentivirus vector with or without cloned transgene along with 9.3 μ g gag-pol expression plasmid pMDLg/pRRE (Plasmid #12251, Addgene, Watertown, MA), 5.4 μ g of Rev. accessory protein plasmid pRSV-REV (Plasmid #12253, Addgene) and 5.4 μ g VSV-G envelope expression plasmid pCMV-VSV-G (Plasmid #8454, Addgene) using FuGene (Promega, Madison, WI). The culture medium was changed 12-16 h post-transfection and the supernatant containing assembled viral particles was collected at 48, 72, and 96 h post-transfection, filtered with low protein binding 0.45 μ m sterile filters, and virus particles concentrated by ultracentrifugation²⁷. Virus titers were determined using 293T cells based on GFP fluorescence using a BD LSR II Flow Cytometer (BD Biosciences, San Jose, CA).

Overexpression and knockdown of CAMKK2:

Primary articular chondrocytes were isolated as mentioned above, from cartilage derived donors without OA (tissue procured from National Disease Research Interchange (NDRI), Philadelphia, PA; see Table 3). P0 chondrocytes were seeded in 6 well plates at 0.8×10^6 /well and incubated overnight at 37 °C/5% CO₂ in CM. Lentiviruses (control, WT or mutant) were added at 5:1 MOI in the presence of the cationic polymer hexadimethrine bromide (polybrene; 4 μ g/ml; Millipore

Sigma). Media was changed after 17 h. Lentivirus transduction efficiency was determined using flow cytometry and transgenic protein expression determined via immunoblotting. For *CAMKK2* knockdown, P0 human articular chondrocytes isolated from healthier intact areas of cartilage were transfected with *CAMKK2* siRNA (ON-TARGET plus Custom SMARTpool; a mixture of 4 siRNA targeting *CAMKK2*; sequence information is proprietary) or scrambled siRNA (both from GE Healthcare Dharmacon, Lafayette, CO; <https://horizondiscovery.com/en/gene-modulation/knockdown/sirna/products/on-targetplus-sirna-reagents?nodeid=entrezgene-10645>), per manufacturer instruction. Protein lysates were prepared 72 h later for downstream analyses.

Immunoblotting:

P0 chondrocyte lysates with equal quantities of protein were fractionated under denaturing conditions on SDS-PAGE and transferred onto on to Immobilon-P membranes (Millipore Sigma®). Blocking, primary antibody, and secondary antibody incubations were performed in Tris-buffered saline (TBS) containing 5% non-fat dry milk. Washes were performed in TBS with Tween-20 (0.1%, v/v, Millipore Sigma). Membranes were probed with primary antibodies listed in Supplementary Table 1 and horseradish peroxidase-conjugated secondary antibodies (Jackson ImmunoResearch Laboratories®, West Grove, PA, USA). Target proteins were visualized with chemiluminescence substrate (Bio-Rad) using a ChemiDox MP Image System (Bio-Rad), and band densities quantified using Image lab (Bio-Rad).

Statistics:

Statistical analyses were performed using the GraphPad Prism software (GraphPad Software, San Diego, CA). Normality assumptions were evaluated using histograms and QQ plots. For normally distributed data, Student's paired t-tests were used where matched data came from different locations on the femoral head of a single individual. Otherwise, groups were compared by student's t-test. For nonparametric data, a Wilcoxon Signed Rank Test was used to compare paired groups with $n = 5$ pairs. For statistical comparisons of 3 groups or more, a one-way analysis of variance was utilized with post-hoc Tukey's HSD for individual groups comparisons where appropriate. Statistical significance was set at $p < 0.05$.

Results:

CAMKK2 and catabolic markers are elevated, and anabolic markers diminished, in human OA cartilage

OARSI scoring of SO-stained sections of paired osteochondral plugs indicated significantly higher grade of cartilage degeneration in the OA portions compared to the intact "healthier" regions of the same femoral head (3.9 vs 1.7, $n=10$ pairs, $p=0.0003$) (Fig. 2). *CAMKK2* mRNA expression was 2-fold higher in OA cartilage compared to healthy tissue ($n=8$, $p=0.025$) (Fig 3A). Further, expression of the catabolic marker *MMP-13* was significantly elevated, whereas that of cartilage anabolic markers *ACAN* and *COL2A1* were diminished in OA cartilage compared to intact samples (Fig. 3A). To assess if the changes in mRNA expression translated to differences in cellular levels of the corresponding proteins, we performed immunostaining of femoral plug sections and found OA cartilage to possess

significantly increased numbers of cells positive for CAMKK2 and MMP-13 (Fig. 3B, Bi, C, Ci). In contrast, COL2A1 positivity was significantly decreased in OA cartilage (Fig. 3D-Di). Thus, OA severity is associated with increased CAMKK2 and MMP13 and diminished COL2A1 levels. We next investigated whether CAMKK2 levels become altered in human chondrocytes following exposure to inflammatory cytokines such as interleukin 1 β (IL-1 β). Treatment with 10 ng/ml recombinant IL-1 β significantly elevated CAMKK2 levels in P0 primary chondrocytes isolated from non-OA cartilage derived from healthy donors (Fig. 3E-3Ei).

OA chondrocytes display increased levels of apoptosis, which is attenuated following CAMKK2 inhibition

Cartilage from the OA portions of the femoral heads displayed increased levels of TUNEL positivity compared to “healthier” intact cartilage, indicating enhanced cell death (n=11 pairs, $p=0.02$, Fig. 4A-Ai). Treatment of OA cartilage explants with the CAMKK2 inhibitor STO-609 resulted in a significant reduction of TUNEL-positive chondrocytes in the OA explants, indicating protection from apoptosis (n=5 pairs, $p=0.0002$ at 24h and 0.0025 at 48 h of treatment, Fig. 4B, Bi). STO-609 treatment inhibits CAMKK2 function, as confirmed by markedly reduced levels of phosphorylated CAMKIV, a canonical CAMKK2 substrate¹⁷ in OA cartilage explants treated with the CAMKK2 inhibitor for 24 hours (n=4, $p=0.0005$) (Fig. 4C-Cii). Further, we observed significantly higher Annexin V positivity in primary articular chondrocytes isolated from OA cartilage compared to those from the healthier portion of the femoral head, indicating increased levels of apoptosis (Fig. D-Di). Treatment with CAMKK2 inhibitor STO-609 for 24 h attenuated apoptosis in OA chondrocytes as evidenced by diminished Annexin V positivity, whereas no significant treatment effects were observed in healthy chondrocytes (Fig. D-Di).

CAMKK2 overexpression upregulates, and its knockdown downregulates, pro-apoptotic, catabolic, and inflammatory protein levels in human articular chondrocytes

Our data thus far indicate that human OA is associated with elevated CAMKK2, and inhibition of the kinase attenuates apoptosis in arthritic chondrocytes. To understand whether CAMKK2 regulates molecular mechanisms coordinating catabolic and apoptotic responses in chondrocytes, we overexpressed the kinase in primary healthy articular chondrocytes, using lentiviruses, or downregulated its expression using siRNA (Fig. 5A-5B, 5H, 5I). AMPK, a key regulator of cell metabolism, is a direct downstream target of CAMKK2 in many cell types including murine chondrocytes^{17, 25, 28}. Indeed, articular chondrocytes overexpressing wild-type (WT) CAMKK2 displayed 2-fold higher phosphorylated (p) AMPK than those transduced with control Lentivirus, whereas over-expression of the kinase-inactive CAMKK2-D311A mutant did not elicit AMPK activation (Fig. 5A, 5C). Conversely, *CAMKK2* knockdown lowered pAMPK levels by 1.8-fold (Fig. 5H, 5J), indicating a key role for CAMKK2 in the basal activation of AMPK in human articular chondrocytes. Chondrocyte apoptosis is mediated by the levels of BAX and BCL-2^{10, 11}, and we next investigated the levels of these proteins following CAMKK2 gain or loss of function in human articular chondrocytes. Compared to chondrocytes transduced with control Lentivirus, cells overexpressing WT CAMKK2, but not the D311A mutant^{25, 26}, possessed 1.5-fold higher levels of the pro-apoptotic protein BAX (Fig. 5A, 5D). In contrast,

CAMKK2 knockdown elicited a 2-fold decrease in BAX compared to control (Fig. 5H, 5K). However, levels of the pro-survival protein BCL-2 was not altered with *CAMKK2* gain and loss of function (Fig. 5A, 5E, 5H, 5L). Altogether, these data indicate that *CAMKK2* is associated with increased BAX expression and enhanced chondrocyte apoptosis, whereas the inhibition of the kinase diminishes BAX and chondrocyte apoptosis.

MMP13 regulates cartilage catabolism in OA²⁹. Since *CAMKK2* is enhanced in OA, we surmised manipulation of its expression in human articular chondrocytes will affect MMP13. Indeed, overexpression of WT *CAMKK2*, not the D311A mutant, significantly increased the levels of chondrocyte-derived MMP13 compared to vector-only control (Fig. 5A, 5F). Knockdown of *CAMKK2* diminished MMP13 by 1.9-fold in chondrocytes (Fig. 5H, 5M), suggesting a key role for *CAMKK2* in cartilage catabolism. Activation of signal transducer and activator of transcription 3 (STAT3) plays a key role in regulating MMP13 expression in inflamed chondrocytes³⁰⁻³³. We previously reported STAT3 activation to be suppressed in *CAMKK2*-deficient murine articular chondrocytes¹⁷, but whether basal STAT3 phosphorylation is altered by *CAMKK2* expression was not clear. Indeed, human articular chondrocytes overexpressing *CAMKK2* possessed significantly higher pSTAT3 than those expressing the *CAMKK2*-D311A mutant or the empty Lentivirus vector (Fig. 5A, 5G). Conversely, knockdown of *CAMKK2* significantly diminished pSTAT3 in human articular chondrocytes (Fig. 5H, 5N). Thus, alteration of *CAMKK2* expression alters STAT3 activation, as well as MMP13 and BAX levels, indicating an important role for the kinase in catabolic and apoptotic mechanisms in human articular chondrocytes.

Discussion

We previously reported a key role for *CAMKK2* in the pathogenesis of murine post-traumatic OA. However, whether the kinase plays a role in human OA remained unknown. Our findings from this study show *CAMKK2* mRNA and protein to be elevated in human OA cartilage. *CAMKK2* levels positively associated with catabolic marker expression and chondrocyte apoptosis, whereas it negatively associated with anabolic marker expression. We further demonstrate that modulation of *CAMKK2* activity led to concordant changes in MMP13, with *CAMKK2* knockdown diminishing and its overexpression enhancing levels of the catabolic protein. MMP13 and cartilage catabolism in OA is mediated through a STAT3-mediated mechanism^{33, 34}. Indeed, levels of pSTAT3 were elevated in human articular chondrocytes overexpressing *CAMKK2* and decreased with its knockdown. In addition to stimulating catabolism, activation of JAK/STAT pathway by the inflammatory cytokine IL-6 leads to the suppression of COL2 and ACAN in articular chondrocytes and cartilage anabolism³⁵, underscoring the vital role played by this pathway in OA pathogenesis. In murine chondrocytes, *CAMKK2* plays a regulatory role in coordinating inflammatory and catabolic responses by stimulating the IL-6-STAT3-MMP13 pathway downstream of IL-1 β , and blocking the kinase protects cartilage anabolism¹⁷. Indeed, treatment of normal (non-OA) human chondrocytes with IL-1 β resulted in a 3-fold increase in *CAMKK2* levels, indicating an inflammation-mediated mechanism upregulating this kinase in OA. We therefore postulate that *CAMKK2* regulates the activation of STAT3/MMP13 pathway downstream of inflammatory cues to facilitate cartilage degradation in human OA.

Chondrocyte apoptosis is a hallmark of human OA^{7-9, 12}, although its causative role in the disease pathogenesis is not clear³⁶. We observed increased TUNEL activity and Annexin V positivity in articular chondrocytes present in OA cartilage. Pharmacological inhibition of CaMKK2 using STO-609 attenuated apoptosis in OA explants and chondrocytes. Moreover, levels of BAX, a key mediator of chondrocyte apoptosis¹¹, were concomitantly enhanced with CAMKK2 overexpression and diminished with its knockdown, indicating a role for CAMKK2 in facilitating BAX-mediated apoptosis of chondrocytes in OA. Whereas the role of CAMKK2 in mediating inflammation in multiple cell types is well-established^{16, 17}, its role in apoptosis is less clear. Consistent with our findings, CAMKK2 has been shown to facilitate triptolide-induced apoptosis in non-small cell lung cancer cells³⁷ and hypoxia-ischemic and oxygen/glucose deprivation induced apoptosis in neonatal neurons through an AMPK-mediated mechanism³⁸. In contrast, CAMKK2 has been shown to promote survival in neurons³⁹⁻⁴¹, ovarian cancer⁴², and cardiac muscle following reperfusion injury⁴³ via its activation of the AMPK and AKT pathways. These differential effects of CAMKK2 on cell survival could depend on the cell type and the nature of injury or treatment. Nevertheless, our findings from this study indicate that CAMKK2 plays a pro-apoptotic role in OA chondrocytes, and its inhibition attenuates cell death.

Overexpression of enzymatically active CAMKK2 in human articular chondrocytes enhanced pAMPK, and its knockdown resulted in the opposite. Since this activation of AMPK occurred in the absence of any external stimuli, such as metformin or IL-1 β , we posit that CAMKK2 is responsible for the basal phosphorylation of AMPK in articular chondrocytes. Indeed, basal pAMPK was lower in CAMKK2-null murine articular chondrocytes¹⁷. AMPK coordinates chondrocyte metabolic regulation⁴⁴, but the exact role of CAMKK2-AMPK pathway in articular chondrocytes is unclear. CAMKK2-AMPK pathway is activated in neonatal neurons undergoing apoptosis following oxygen/glucose deprivation, and inhibition of AMPK enhances their survival³⁸. Thus, pathogenic activation of CAMKK2-AMPK in OA chondrocytes could elicit apoptosis and cartilage catabolism through BAX and STAT3-MMP13 mediated mechanisms.

Much of the upregulated CAMKK2 in OA is observed in the superficial zone, inclusive of the tangential and transitional layers of cartilage (Fig. 3B)¹⁷. Advanced OA (KL grade 2.5 and higher) results in the loss of much of this layer, resulting in the large variation in CAMKK2 mRNA and protein levels in the OA cartilage, as we observed (Fig. 3A-B). For these reasons, we utilized healthy cartilage from non-OA donors for the CAMKK2 loss and gain-of-function experiments to evaluate downstream mechanism (Fig. 5). We speculate based on our cumulative data that CAMKK2 is involved in the early OA pathogenic processes in chondrocytes.

One limitation of our study is that the “healthy” cartilage was taken from areas without macroscopic arthritis from the same OA femoral heads. While this allowed for “paired” comparison from the same sample, prior studies have shown that this “healthy” intact cartilage tissue can have higher levels of IL-1 β expression and proteoglycan loss than cartilage taken from non-arthritic joints⁴⁵. Despite this limitation, we still observed significant differences in all studied markers between cartilage samples taken from the same joint. Moreover, both the histology and the OARSI scores suggest cartilage in the posterior-

lateral region of the femoral head are “healthier” than those in the region with established OA (Fig. 2). Future studies comparing truly healthy cartilage may further bolster the results seen in the current study. Another potential limitation is that our study was performed on established human OA samples, and so the effects of CAMKK2 on OA pathogenesis could not be evaluated. In the clinical setting however, patients present for OA treatment when they are symptomatic (pain) and have advanced disease.

In conclusion, our findings show that CAMKK2 is involved in catabolic and apoptotic responses in human primary chondrocytes, potentially through STAT3/MMP13 and BAX-mediated mechanisms. Blocking CAMKK2 activity or expression reduced chondrocyte apoptosis and catabolic protein expression. Although the exact mechanism by which CAMKK2 modulates inflammatory, catabolic, and apoptotic pathways in human primary OA remains to be investigated, our findings identify CAMKK2 as a promising therapeutic target in the treatment of established primary OA, which currently has no clinical disease modifying treatments.

Supplementary Material

Refer to Web version on PubMed Central for supplementary material.

Acknowledgments

The authors thank Dr. Ziyue Liu, Associate Professor of Biostatistics & Health Data Sciences, IUSM for help with statistical analysis, and Drew M. Brown and the staff at the Musculoskeletal Histology Core Facility of the Indiana Center for Musculoskeletal Health and the Bone and Body Composition Core of the Indiana Clinical Translational Sciences Institute (CTSI) for help with histology and guidance on immunohistochemistry.

Funding source

This study was supported by DoD Peer Reviewed Medical Research Program – Investigator-Initiated Research Award W81XWH-20-1-0304 from the U.S. ARMY MEDICAL RESEARCH ACQUISITION ACTIVITY and NIAMS/NIH R01AR076477. JED and AS were supported through a Comprehensive Musculoskeletal T32 Training Program from NIAMS/NIH (AR065971). MB was supported by the Indiana Clinical and Translational Sciences Institute which is funded in part by National Institutes of Health, National Center for Advancing Translational Sciences, Clinical and Translational Sciences Award (Award Number UL1TR002529). The study sponsors were not involved in any aspects of this study including study design, collection, analysis, and interpretation of data; or in the writing of the manuscript, and in the decision to submit the manuscript for publication. The content is solely the responsibility of the authors and does not necessarily represent the official views of the National Institutes of Health.

References:

1. Litwic A, Edwards MH, Dennison EM, Cooper C. Epidemiology and burden of osteoarthritis. *Br Med Bull.* 2013;105:185–99. Epub 2013/01/23. doi: 10.1093/bmb/lds038. [PubMed: 23337796]
2. Pasquale MK, Louder AM, Cheung RY, Reiners AT, Mardekian J, Sanchez RJ, et al. Healthcare Utilization and Costs of Knee or Hip Replacements versus Pain-Relief Injections. *Am Health Drug Benefits.* 2015;8(7):384–94. Epub 2015/11/12. [PubMed: 26557232]
3. Yao JJ, Hevesi M, Visscher SL, Ransom JE, Lewallen DG, Berry DJ, et al. Direct Inpatient Medical Costs of Operative Treatment of Periprosthetic Hip and Knee Infections Are Twofold Higher Than Those of Aseptic Revisions. *J Bone Joint Surg Am.* 2021;103(4):312–8. Epub 2020/12/01. doi: 10.2106/JBJS.20.00550. [PubMed: 33252589]
4. Chen D, Shen J, Zhao W, Wang T, Han L, Hamilton JL, et al. Osteoarthritis: toward a comprehensive understanding of pathological mechanism. *Bone Res.* 2017;5:16044. Epub 2017/02/06. doi: 10.1038/boneres.2016.44. [PubMed: 28149655]

5. Robinson WH, Lepus CM, Wang Q, Raghu H, Mao R, Lindstrom TM, et al. Low-grade inflammation as a key mediator of the pathogenesis of osteoarthritis. *Nat Rev Rheumatol*. 2016;12(10):580–92. Epub 2016/08/20. doi: 10.1038/nrrheum.2016.136. [PubMed: 27539668]
6. Perez-Garcia S, Carrion M, Gutierrez-Canas I, Villanueva-Romero R, Castro D, Martinez C, et al. Profile of Matrix-Remodeling Proteinases in Osteoarthritis: Impact of Fibronectin. *Cells*. 2019;9(1). Epub 2019/12/28. doi: 10.3390/cells9010040.
7. Hashimoto S, Ochs RL, Komiya S, Lotz M. Linkage of chondrocyte apoptosis and cartilage degradation in human osteoarthritis. *Arthritis Rheum*. 1998;41(9):1632–8. Epub 1998/09/29. doi: 10.1002/1529-0131(199809)41:9<1632::AID-ART14>3.0.CO;2-A. [PubMed: 9751096]
8. Heraud F, Heraud A, Harmand MF. Apoptosis in normal and osteoarthritic human articular cartilage. *Ann Rheum Dis*. 2000;59(12):959–65. Epub 2000/11/23. doi: 10.1136/ard.59.12.959. [PubMed: 11087699]
9. Thomas CM, Fuller CJ, Whittles CE, Sharif M. Chondrocyte death by apoptosis is associated with the initiation and severity of articular cartilage degradation. *Int J Rheum Dis*. 2011;14(2):191–8. Epub 2011/04/27. doi: 10.1111/j.1756-185X.2010.01578.x. [PubMed: 21518319]
10. Campbell KJ, Tait SWG. Targeting BCL-2 regulated apoptosis in cancer. *Open Biol*. 2018;8(5). Epub 2018/05/18. doi: 10.1098/rsob.180002.
11. Miao G, Zang X, Hou H, Sun H, Wang L, Zhang T, et al. Bax Targeted by miR-29a Regulates Chondrocyte Apoptosis in Osteoarthritis. *Biomed Res Int*. 2019;2019:1434538. Epub 2019/04/18. doi: 10.1155/2019/1434538. [PubMed: 30993110]
12. Aigner T, Kim HA. Apoptosis and cellular vitality: issues in osteoarthritic cartilage degeneration. *Arthritis Rheum*. 2002;46(8):1986–96. Epub 2002/09/05. doi: 10.1002/art.10554. [PubMed: 12209500]
13. Bobinac D, Spanjol J, Zoricic S, Maric I. Changes in articular cartilage and subchondral bone histomorphometry in osteoarthritic knee joints in humans. *Bone*. 2003;32(3):284–90. Epub 2003/04/02. doi: 10.1016/s8756-3282(02)00982-1. [PubMed: 12667556]
14. Williams JN, Sankar U. CaMKK2 Signaling in Metabolism and Skeletal Disease: a New Axis with Therapeutic Potential. *Curr Osteoporos Rep*. 2019;17(4):169–77. Epub 2019/05/23. doi: 10.1007/s11914-019-00518-w. [PubMed: 31115859]
15. Anderson KA, Ribar TJ, Lin F, Noeldner PK, Green MF, Muehlbauer MJ, et al. Hypothalamic CaMKK2 contributes to the regulation of energy balance. *Cell Metab*. 2008;7(5):377–88. Epub 2008/05/08. doi: 10.1016/j.cmet.2008.02.011. [PubMed: 18460329]
16. Racioppi L, Noeldner PK, Lin F, Arvai S, Means AR. Calcium/calmodulin-dependent protein kinase kinase 2 regulates macrophage-mediated inflammatory responses. *J Biol Chem*. 2012;287(14):11579–91. Epub 2012/02/16. doi: 10.1074/jbc.M111.336032. [PubMed: 22334678]
17. Mevel E, Shutter JA, Ding X, Mattingly BT, Williams JN, Li Y, et al. Systemic inhibition or global deletion of CaMKK2 protects against post-traumatic osteoarthritis. *Osteoarthritis Cartilage*. 2022;30(1):124–36. Epub 2021/09/11. doi: 10.1016/j.joca.2021.09.001. [PubMed: 34506942]
18. Kellgren JH, Lawrence JS. Radiological assessment of osteo-arthrosis. *Ann Rheum Dis*. 1957;16(4):494–502. Epub 1957/12/01. doi: 10.1136/ard.16.4.494. [PubMed: 13498604]
19. Pritzker KP, Gay S, Jimenez SA, Ostergaard K, Pelletier JP, Revell PA, et al. Osteoarthritis cartilage histopathology: grading and staging. *Osteoarthritis Cartilage*. 2006;14(1):13–29. Epub 2005/10/26. doi: 10.1016/j.joca.2005.07.014. [PubMed: 16242352]
20. Waldstein W, Perino G, Gilbert SL, Maher SA, Windhager R, Boettner F. OARSI osteoarthritis cartilage histopathology assessment system: A biomechanical evaluation in the human knee. *J Orthop Res*. 2016;34(1):135–40. Epub 2015/08/08. doi: 10.1002/jor.23010. [PubMed: 26250350]
21. Pauli C, Whiteside R, Heras FL, Nestic D, Koziol J, Grogan SP, et al. Comparison of cartilage histopathology assessment systems on human knee joints at all stages of osteoarthritis development. *Osteoarthritis and Cartilage*. 2012;20(6):476–85. doi: 10.1016/j.joca.2011.12.018. [PubMed: 22353747]
22. Pearson RG, Kurien T, Shu KSS, Scammell BE. Histopathology grading systems for characterisation of human knee osteoarthritis – reproducibility, variability, reliability, correlation, and validity. *Osteoarthritis and Cartilage*. 2011;19(3):324–31. doi: 10.1016/j.joca.2010.12.005. [PubMed: 21172446]

23. Valiya Kambrath A, Williams JN, Sankar U. An Improved Methodology to Evaluate Cell and Molecular Signals in the Reparative Callus During Fracture Healing. *J Histochem Cytochem*. 2020;68(3):199–208. Epub 2020/01/14. doi: 10.1369/0022155419900915. [PubMed: 31928129]
24. Livak KJ, Schmittgen TD. Analysis of relative gene expression data using real-time quantitative PCR and the 2⁻($\Delta\Delta C_T$) Method. *Methods*. 2001;25(4):402–8. Epub 2002/02/16. doi: 10.1006/meth.2001.1262. [PubMed: 11846609]
25. Green MF, Anderson KA, Means AR. Characterization of the CaMKK β -AMPK signaling complex. *Cell Signal*. 2011;23(12):2005–12. Epub 2011/08/03. doi: 10.1016/j.cellsig.2011.07.014. [PubMed: 21807092]
26. Green MF, Scott JW, Steel R, Oakhill JS, Kemp BE, Means AR. Ca²⁺/Calmodulin-dependent protein kinase kinase β is regulated by multisite phosphorylation. *J Biol Chem*. 2011;286(32):28066–79. Epub 2011/06/15. doi: 10.1074/jbc.M111.251504. [PubMed: 21669867]
27. Todd LR, Damin MN, Gomathinayagam R, Horn SR, Means AR, Sankar U. Growth factor *erv1*-like modulates Drp1 to preserve mitochondrial dynamics and function in mouse embryonic stem cells. *Mol Biol Cell*. 2010;21(7):1225–36. Epub 2010/02/12. doi: 10.1091/mbc.e09-11-0937. [PubMed: 20147447]
28. Hurley RL, Anderson KA, Franzone JM, Kemp BE, Means AR, Witters LA. The Ca²⁺/calmodulin-dependent protein kinase kinases are AMP-activated protein kinase kinases. *J Biol Chem*. 2005;280(32):29060–6. Epub 2005/06/28. doi: 10.1074/jbc.M503824200. [PubMed: 15980064]
29. Burrage PS, Mix KS, Brinckerhoff CE. Matrix metalloproteinases: role in arthritis. *Front Biosci*. 2006;11:529–43. Epub 2005/09/09. doi: 10.2741/1817. [PubMed: 16146751]
30. Akeson G, Malemud CJ. A Role for Soluble IL-6 Receptor in Osteoarthritis. *J Funct Morphol Kinesiol*. 2017;2(3):27. Epub 2017/08/02. doi: 10.3390/jfmk2030027. [PubMed: 29276788]
31. Wiegertjes R, van de Loo FAJ, Blaney Davidson EN. A roadmap to target interleukin-6 in osteoarthritis. *Rheumatology*. 2020;59(10):2681–94. doi: 10.1093/rheumatology/keaa248. [PubMed: 32691066]
32. Sherwood JC, Bertrand J, Eldridge SE, Dell'Accio F. Cellular and molecular mechanisms of cartilage damage and repair. *Drug Discovery Today*. 2014;19(8):1172–7. doi: 10.1016/j.drudis.2014.05.014. [PubMed: 24880104]
33. Latourte A, Cherifi C, Maillet J, Ea HK, Bouaziz W, Funck-Brentano T, et al. Systemic inhibition of IL-6/Stat3 signalling protects against experimental osteoarthritis. *Ann Rheum Dis*. 2017;76(4):748–55. Epub 2016/11/01. doi: 10.1136/annrheumdis-2016-209757. [PubMed: 27789465]
34. Aida Y, Honda K, Tanigawa S, Nakayama G, Matsumura H, Suzuki N, et al. IL-6 and soluble IL-6 receptor stimulate the production of MMPs and their inhibitors via JAK-STAT and ERK-MAPK signalling in human chondrocytes. *Cell Biol Int*. 2012;36(4):367–76. Epub 2011/11/18. doi: 10.1042/CBI20110150. [PubMed: 22087578]
35. Legendre F, Dudhia J, Pujol J-P, Bogdanowicz P. JAK/STAT but Not ERK1/ERK2 Pathway Mediates Interleukin (IL)-6/Soluble IL-6R Down-regulation of Type II Collagen, Aggrecan Core, and Link Protein Transcription in Articular Chondrocytes: ASSOCIATION WITH A DOWN-REGULATION OF SOX9 EXPRESSION*. *Journal of Biological Chemistry*. 2003;278(5):2903–12. doi: 10.1074/jbc.M110773200. [PubMed: 12419823]
36. Zhang M, Mani SB, He Y, Hall AM, Xu L, Li Y, et al. Induced superficial chondrocyte death reduces catabolic cartilage damage in murine posttraumatic osteoarthritis. *J Clin Invest*. 2016;126(8):2893–902. Epub 2016/07/18. doi: 10.1172/jci83676. [PubMed: 27427985]
37. Ren T, Tang YJ, Wang MF, Wang HS, Liu Y, Qian X, et al. Triptolide induces apoptosis through the calcium/calmodulin-dependent protein kinase β /AMP-activated protein kinase signaling pathway in non-small cell lung cancer cells. *Oncol Rep*. 2020;44(5):2288–96. Epub 2020/10/02. doi: 10.3892/or.2020.7763. [PubMed: 33000264]
38. Rousset CI, Leiper FC, Kichev A, Gressens P, Carling D, Hagberg H, et al. A dual role for AMP-activated protein kinase (AMPK) during neonatal hypoxic-ischaemic brain injury in mice. *J Neurochem*. 2015;133(2):242–52. Epub 2015/01/20. doi: 10.1111/jnc.13034. [PubMed: 25598140]

39. Zhang Y, Xu N, Ding Y, Doycheva DM, Zhang Y, Li Q, et al. Chemerin reverses neurological impairments and ameliorates neuronal apoptosis through ChemR23/CAMKK2/AMPK pathway in neonatal hypoxic-ischemic encephalopathy. *Cell Death Dis.* 2019;10(2):97. Epub 2019/02/06. doi: 10.1038/s41419-019-1374-y. [PubMed: 30718467]
40. Zhang Y, Zhang P, Deng C. miR-378a-5p regulates CAMKK2/AMPK pathway to contribute to cerebral ischemia/reperfusion injury-induced neuronal apoptosis. *Folia Histochem Cytobiol.* 2021;59(1):57–65. Epub 2021/03/03. doi: 10.5603/FHC.a2021.0007. [PubMed: 33651374]
41. Min JW, Bu F, Qi L, Munshi Y, Kim GS, Marrelli SP, et al. Inhibition of Calcium/Calmodulin-Dependent Protein Kinase Kinase beta Is Detrimental in Hypoxia(-)Ischemia Neonatal Brain Injury. *Int J Mol Sci.* 2019;20(9). Epub 2019/04/28. doi: 10.3390/ijms20092063.
42. Gocher AM, Azabdaftari G, Euscher LM, Dai S, Karacosta LG, Franke TF, et al. Akt activation by Ca(2+)/calmodulin-dependent protein kinase kinase 2 (CaMKK2) in ovarian cancer cells. *J Biol Chem.* 2017;292(34):14188–204. Epub 2017/06/22. doi: 10.1074/jbc.M117.778464. [PubMed: 28634229]
43. Qi D, Atsina K, Qu L, Hu X, Wu X, Xu B, et al. The vestigial enzyme D-dopachrome tautomerase protects the heart against ischemic injury. *J Clin Invest.* 2014;124(8):3540–50. Epub 2014/07/02. doi: 10.1172/JCI73061. [PubMed: 24983315]
44. Liu-Bryan R. Inflammation and intracellular metabolism: new targets in OA. *Osteoarthritis and cartilage.* 2015;23(11):1835–42. Epub 2015/11/03. doi: 10.1016/j.joca.2014.12.016. [PubMed: 26521729]
45. Weaver RE, Sharif M, Livingston LA, Andrews KL, Fuller CJ. Microscopic change in macroscopically normal equine cartilage from osteoarthritic joints. *Connect Tissue Res.* 2006;47(2):92–101. Epub 2006/06/07. doi: 10.1080/03008200600584165. [PubMed: 16754515]

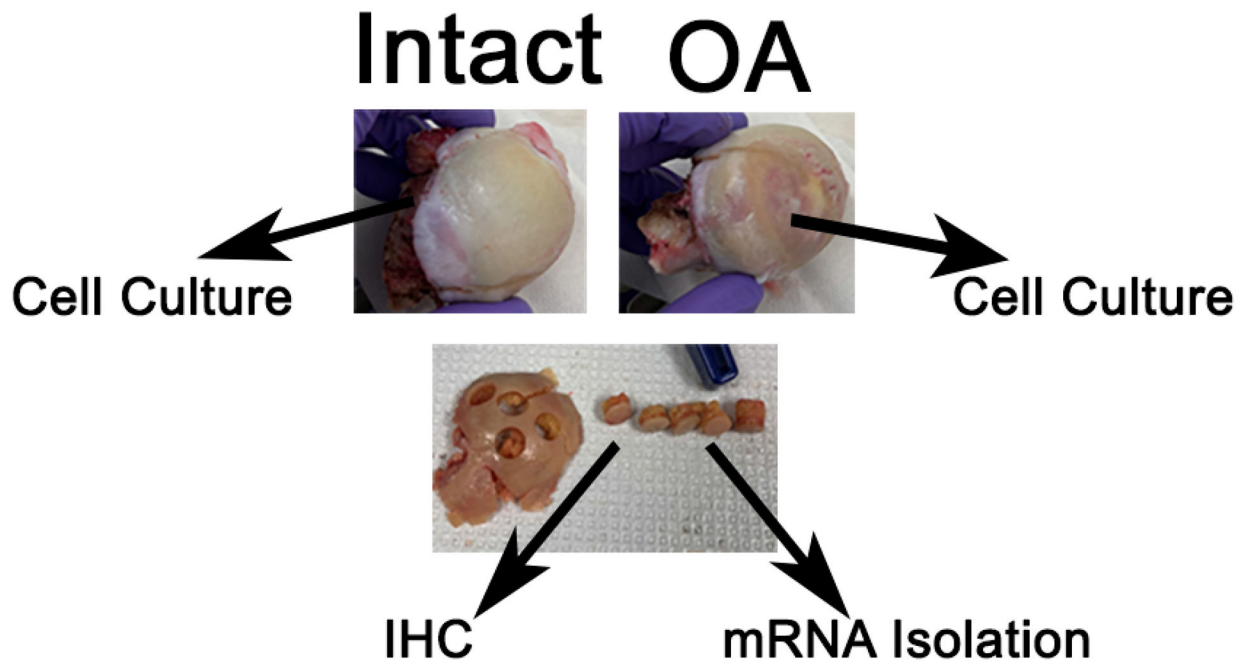


Figure 1. Schematic of “paired” cartilage isolation and osteochondral plug extraction from human femur heads.

(Top) Cartilage isolated from “healthier” intact and OA sides of the same femoral head were used in cell culture-based experiments. **(Bottom)** Example of the osteochondral femoral plugs extracted from intact and OA regions of the same femur head. Two plugs per region were extracted for immunohistochemistry and mRNA analysis.

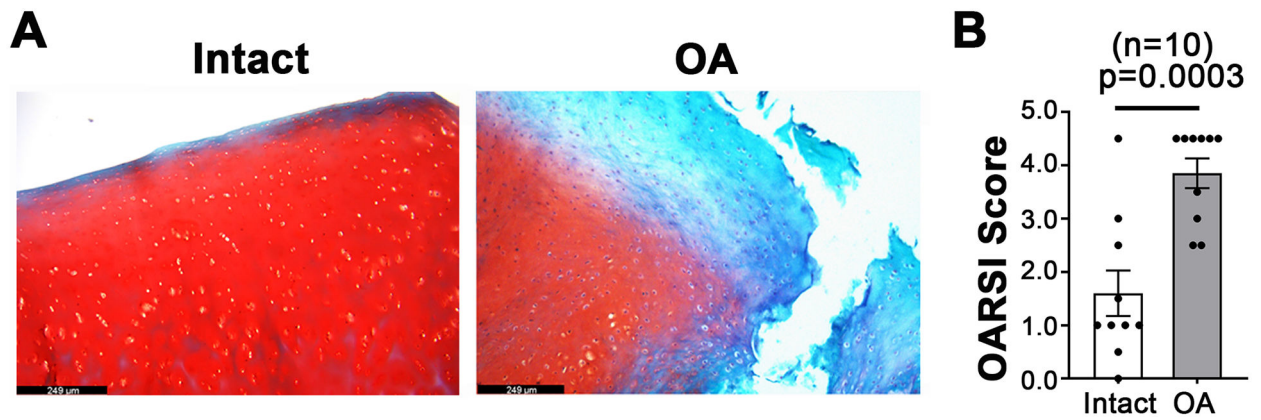


Figure 2. Increased OA severity in femoral plugs isolated from weight bearing portion of the femoral head.

(A) Representative images of paired osteochondral sections of plugs taken from intact and OA portions of the same femoral head stained with safranin O fast green. (100X; Scale bar = 249 µm). (B) OA severity assessed using the histological OARSIS scoring system (n = 10 pairs). Error bars = SD; *p*-value representative of paired student's *t*-test.

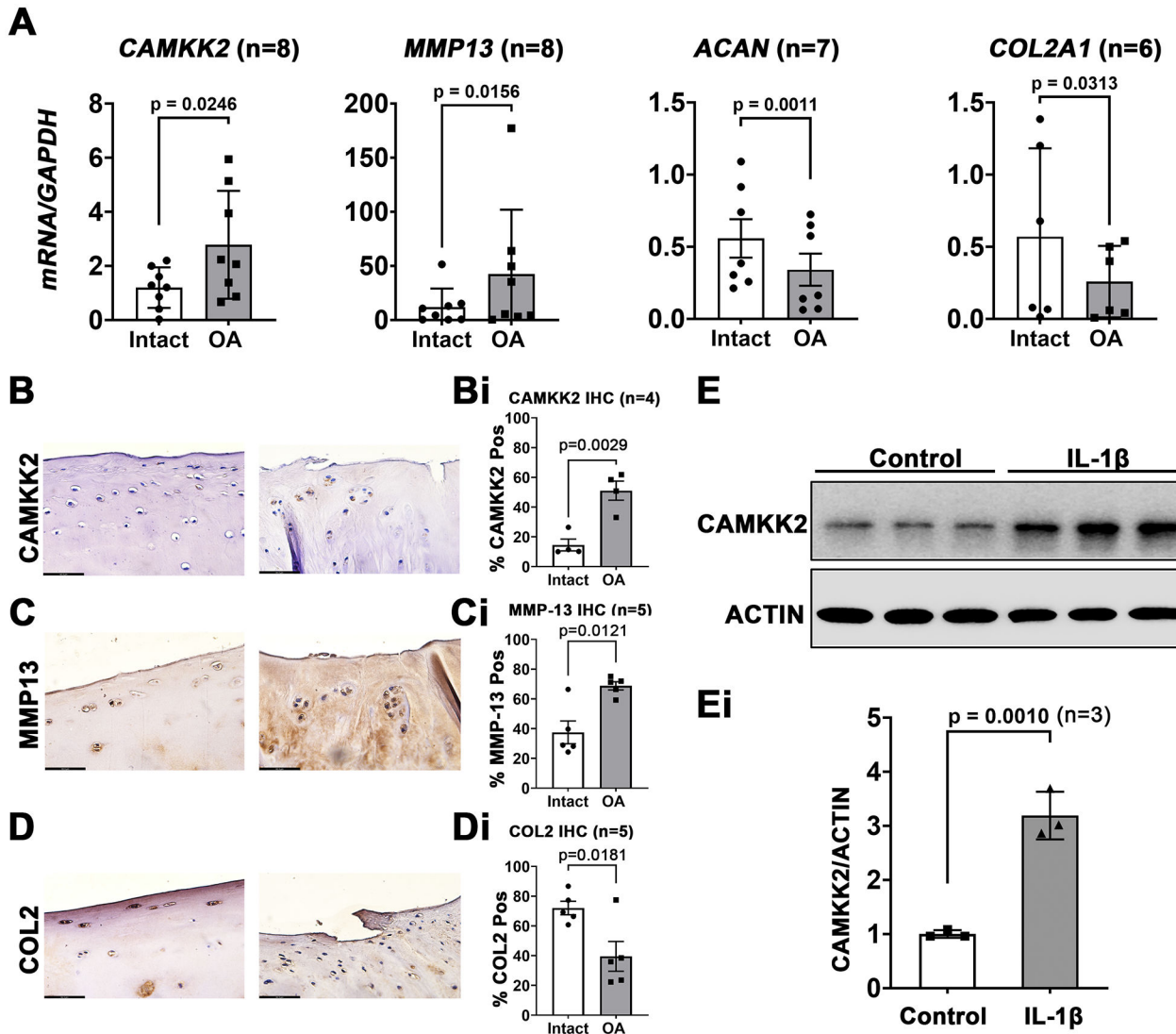


Figure 3. Elevated levels of CAMKK2 and MMP13, and decreased levels of anabolic markers in OA cartilage.

(A) mRNA expression (normalized to *GADPH*) of *CAMKK2*, *MMP13*, *ACAN*, and *COL2A1* in intact and OA femoral head plugs (n=6-8/group). (B, C, D) Representative IHC images indicating immunopositivity to CAMKK2, MMP-13 and COL2 in “paired” intact and OA osteochondral sections (100X, scale bar=62.3 μ m; n=4-5/group). (Bi, Ci, Di) Quantification of CAMKK2, MMP13 and COL2A1 positivity based on IHC images (n=4-5) Error bars = SD. Loss of superficial zone cartilage in the OA cartilage of KL Score >2 affected CAMKK2 expression, and hence the lower N. Paired student’s t-test was used to derive the *p*-value for *CAMKK2* mRNA comparison. Wilcoxon signed-rank test was used for *MMP13* (n=8), *ACAN* (n=8), and *COL2A1* (n=6) mRNA comparisons, *p*-values of IHC were derived using unpaired student’s t-test. (E) Immunoblots from P0 chondrocytes isolated from healthy donors treated with 1X PBS (Control) or 10 ng/ml IL-1 β for 24 h probed for CAMKK2 and ACTIN (loading control) immunoreactivity. Each lane represents lysates from an individual donor, indicating a biological replicate (n=3). (Ei)

Ratio of average signal intensity of CAMKK2 to ACTIN (n=3 biological replicates/group).
Error bars = SD; paired student's t-test was used to derive the *p*-value.

Author Manuscript

Author Manuscript

Author Manuscript

Author Manuscript

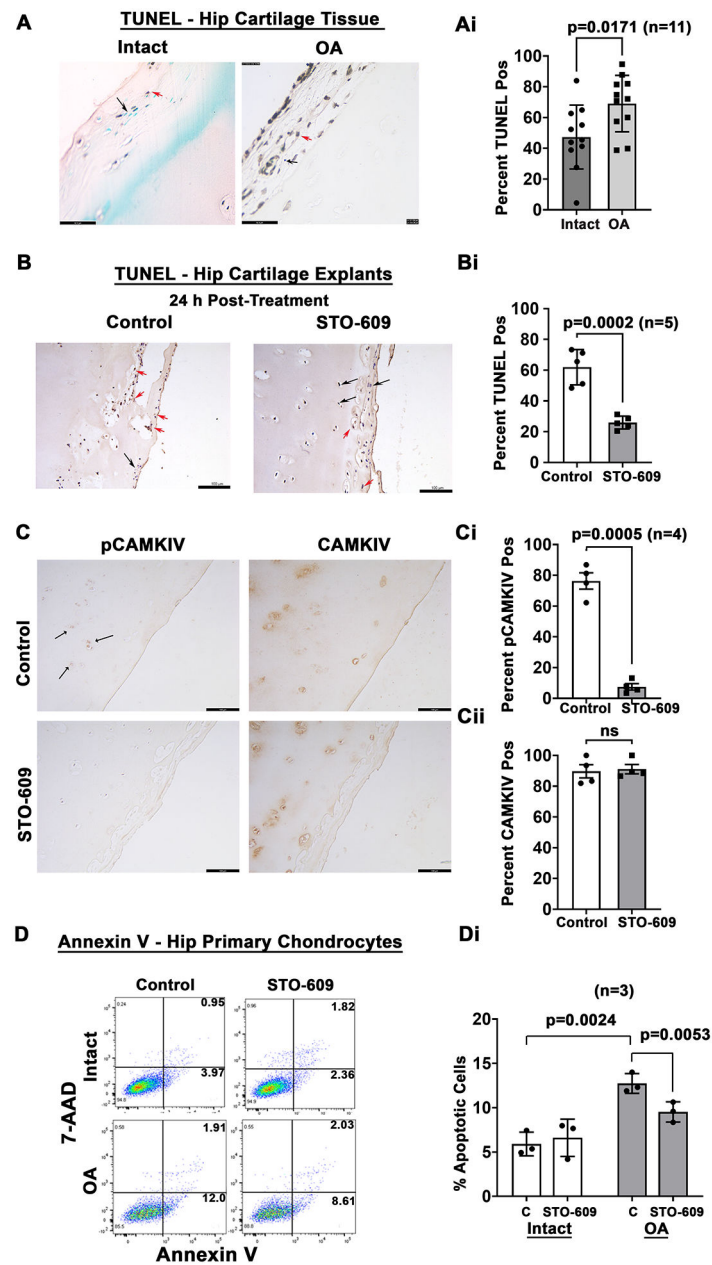


Figure 4. Increased levels of apoptosis in OA chondrocytes, which is attenuated with CAMKK2 inhibition.

(A) Representative sections of TUNEL-stained “paired” intact and OA femoral head plugs showing TUNEL positive (red arrow) and negative (black arrow) cells (100X, 62.3 μ m scale bar). (Ai) Quantification of TUNEL positivity from “paired intact and OA femoral head osteochondral sections (n = 11/group). Error bars = SD; *p*-values assessed using paired student’s t-test. (B-Bi) Representative TUNEL-stained images of OA cartilage explants treated with 1X PBS (Control) or 8 μ M STO-609 for 24 h. (Bi) . Quantification of TUNEL positivity at 24 h post-treatment from the 10 “paired” osteochondral cores (from 5 individual patients – see Table 2) in respective control and STO-609 treated OA cartilage explants (n=5 pairs/cohort; TUNEL positive (red arrow) and negative (black arrow)). Error bars = SD;

paired student's t-test was used to derive the p -value. **(C-Cii)** Representative IHC stained images of OA cartilage explants treated with 1X PBS (Control) or 8 μ M STO-609 for 24 h, showing immunoreactivity to phospho (p) CAMKIV or total CAMKIV. CAMKIV is a canonical substrate of CAMKK2, and hence its phosphorylation status is used as a read out for the inhibition of CAMKK2 activity using STO-609. **(Ci)** Quantification of (Ci) CAMKIV and (Cii) pCAMKIV positivity in control and STO-609 treated OA cartilage explants (n=4 individual explants/cohort). Error bars = SD; paired student's t-test was used to derive the p -value. **(D-Di)** Representative flow cytometry histograms of chondrocytes isolated from paired "healthier" intact and OA regions of the same femoral head, treated with or without (D) the CAMKK2 inhibitor STO-609 for 24 h, and stained for Annexin V-PE and 7-AAD. Annexin V labels apoptotic cells and 7-AAD stains DNA. **(Di)** Percentage apoptotic cells in chondrocytes isolated from paired "healthier" intact and OA cartilage (KL grade = 2) and treated with or without (C) STO-609. Annexin V-positive/7-AAD-negative (early apoptotic) as well as Annexin V-positive/7-AAD-positive (late apoptotic) populations were combined to arrive at % apoptotic cells (n = 3 biological replicates/group). Error bars = SD. The p -values were derived from paired student's t-test comparisons.

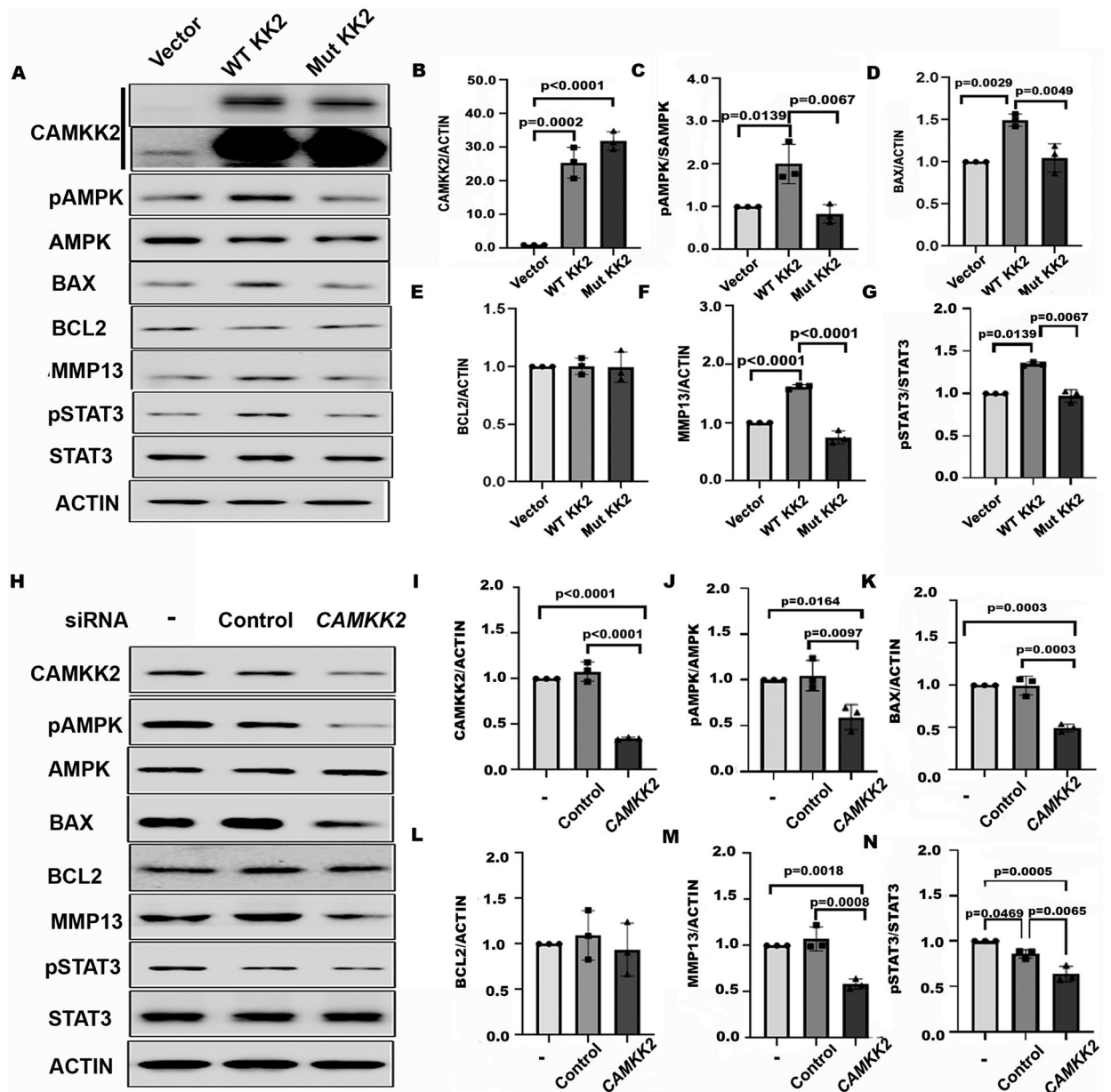


Figure 5. CAMKK2 modulates AMPK and STAT3 activation as well as BAX and MMP-13 levels in human chondrocytes.

(A) Immunoblots of cell extracts from healthy human chondrocytes infected with lentiviral vector (vector) or Lentiviruses expressing CAMKK2 (WT KK2) or a kinase-dead CAMKK2 mutant (Mut KK2) were probed for CAMKK2, phospho- and total AMPK, BAX, BCL2, MMP13, phospho- and total STAT3, and ACTIN. **(B-G)** Average signal intensities of the indicated proteins. **(H)** Immunoblots of cell extracts from naïve healthy human chondrocytes or those transfected with scrambled siRNA (control) or *CAMKK2* siRNA (SMARTpool mix of 4 siRNAs), and probed for CAMKK2, phospho- and total AMPK, BAX, BCL2, MMP13, phospho- and total STAT3, and ACTIN. **(I-N)** Average signal intensities of the indicated proteins. **(B-G; I-N)** The ratio of phosphoprotein band intensities normalized to their respective proteins (pAMPK and pSTAT3) or total protein band intensities over the levels

of B-ACTIN (CAMKK2, BAX, BCL2, and MMP13) are shown. (A-N) Representative blots and quantification from n=3 independent experiments which are three biological replicates are shown. Error bars = SD. The *p*-values were derived by one-way ANOVA followed by Tukey's HSD post-hoc tests.

Author Manuscript

Author Manuscript

Author Manuscript

Author Manuscript

Table 1.

Patient demographic details for de-identified human THA OA cartilage samples used in this study.

I.D.	Age	Sex	Kellgren-Lawrence (KL) Grade
1	53	F	2
2	52	M	3
3	55	F	2
4	50	F	2
5	44	F	2
6	63	M	3
7	63	M	3
8	76	M	2
9	62	F	2
10	46	M	2
11	51	F	2
12	63	F	3

Author Manuscript

Author Manuscript

Author Manuscript

Author Manuscript

Table 2.

Patient demographic details for de-identified human THA OA cartilage samples used in this study for explant culture.

ID	Age	Sex	Kellgren-Lawrence (KL) Grade
1	57	F	2
2	62	F	2
3	57	M	2
4	70	M	3
5	43	M	2

Author Manuscript

Author Manuscript

Author Manuscript

Author Manuscript

Table 3:

Details of donor demographics of non-OA cartilage used for cell culture experiments in this study.

ID	Age	Sex
1	55	M
2	55	M
3	53	M
4	49	F
5	31	F

Author Manuscript

Author Manuscript

Author Manuscript

Author Manuscript